

DOI: doi.org/10.21009/SPEKTRA.101.06

Coordinative Study of Organic Material on Silver Nanoparticles and Its Application for Colorimetric Sensor

Setiya Rahayu¹, Yoda Taruna Hidayah¹, Qoid Abrori Syakuro¹, Azza Azahra Ronald¹, Herman¹, Priastuti Wulandari^{1,*}

¹Physics of Magnetism and Photonics Research Division, Faculty of Mathematics and Natural Sciences, Institut Teknologi Bandung

*Corresponding Author Email: pwulandari@itb.ac.id

Received: 26 December 2024

Revised: 16 April 2025

Accepted: 22 April 2024

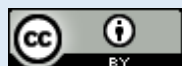
Online: 30 April 2025

Published: 30 April 2025

SPEKTRA: Jurnal Fisika dan Aplikasinya

p-ISSN: 2541-3384

e-ISSN: 2541-3392



ABSTRACT

Metal nanoparticles, especially gold and silver nanoparticles, have been applied in various fields of nanotechnology because of their unique optical properties called localized surface plasmon resonance (LSPR). Metal nanoparticles need capping material to stabilize and protect the metal core. The interaction between capping and metal core affects the physical and chemical properties of metal nanoparticles. Silver nanoparticles have a robust extinction coefficient compared to other metals of the same size. In addition, silver nanoparticles have been found to have antimicrobial properties. There has been a lot of research on the coordination between organic molecules with silver metal. However, the study about the coordination between organic molecules on silver nanoparticles has not been studied in detail. For this reason, the synthesis of silver nanoparticles capped by citrate (AgCA) and silver nanoparticles capped by 3-MPA (AgMPA) was optimized in order to form stable colloids. The interaction between capping molecules (citrate and 3-MPA) and silver core was studied experimentally and computationally. In the results, some different vibration peak positions of chemical coordination between free carboxylate and the carboxylate on silver nanoparticles were found, indicating the effect of strong chemical bonding and the effect of localized surface plasmon. Agreement was found between the experimental results and the calculation based on DFT simulation, which shows the same tendencies of vibration peak position. Moreover, colorimetric testing with Biocytin-Avidin was performed as a sensor application in the experiment.

Keywords: silver nanoparticles, localized surface plasmon resonance, organic capping material, colorimetric sensor

INTRODUCTION

Recent advancements in nanotechnology have significantly expanded the applications of nanoparticles. These domains encompass healthcare, education, and construction. Nanoparticles, such as gold and silver, are extensively utilized in biomedicine for targeted medication delivery techniques. This technique enhances medication bioavailability and reduces overall bodily damage, particularly benefiting cancer treatment and the development of antibacterial agents [1, 2]. The integration of metal-based nanoparticles into manufactured nanofibers has shown promising results in wound healing, promoting tissue regeneration and decreasing the risk of infection [3, 4]. Nanoparticles have enabled the advancement of innovative testing procedures, especially biosensing technologies that can rapidly and accurately identify viruses and biomolecules [1, 5, 6]. In engineering, they are utilized to produce advanced paints and composites that enhance the strength and durability of structural components [7, 8]. Magnetic nanoparticles have significantly enhanced the energy efficiency of heating systems, underscoring their importance across several domains [9, 10].

Metal nanoparticles, especially gold (AuNPs) and silver (AgNPs), are commonly employed in nanotechnology due to their distinctive electrical, chemical, and optical characteristics resulting from localized surface plasmon resonance (LSPR). The interaction between an electromagnetic field and metal nanoparticles induces collective oscillations of surface electrons in the conduction band, leading to distinctive absorption and scattering in the UV-visible spectrum [11–14]. The plasmon resonance of these nanoparticles is often in the visible area, allowing for real-time monitoring of surface changes via color shifts, which is very important in colorimetric sensing applications.

The features of LSPR are influenced by several parameters, including nanoparticle shape, size, surrounding dielectric medium, interparticle distance, and surface functionalization [15, 16]. Organic capping compounds are frequently employed to stabilize colloidal metal nanoparticles and inhibit aggregation, while also enabling alterations to their physical and chemical characteristics, thus rendering them appropriate for various applications [17, 18]. Alterations in the dielectric medium around nanoparticles can induce shifts in the localized surface plasmon resonance (LSPR) peak, leading to observable color changes that are extensively utilized in colorimetric sensors for the detection of particular analytes [14].

The surface functionalization of nanoparticles with capping ligands markedly enhances their efficacy as selective and sensitive detection probes. Mahjub et al. [13] created an aptamer-conjugated silver nanoparticle sensor for the detection of tobramycin (TOB) in milk. The sensor's response is predicated on the interaction between AgNPs and poly A-tailed aptamers, resulting in a color change from 400 nm to 540 nm upon TOB binding. Sekar et al. [19] employed glucose-functionalized gold nanoparticles to identify bacterial presence, observing a linear increase in color intensity according to microbial concentration, thus illustrating the efficacy of these sensors in both solid and liquid phases.

Nanoparticles are essential in enhancing diagnostic methodologies, with LSPR-based sensors demonstrating significant potential in identifying biomolecules and infections. Gold nanorods and nanoshells have demonstrated an ability to augment the sensitivity of LSPR-based sensors,

rendering them appropriate for swift pathogen detection [20, 21]. The utilization of nanoparticles in engineering is expanding, leading to the creation of multifunctional materials that enhance features including conductivity, biocompatibility, and mechanical strength for diverse technological applications [7, 8].

The potential of nanoparticles for use in environmental monitoring and diagnostics has been further expanded by recent advancements in LSPR-based colorimetric sensors. The LSPR peak shifts, which are caused by changes in the refractive index during analyte binding, facilitate visual identification of specific analytes, including heavy metals and microorganisms. Consequently, these sensors are particularly advantageous for rapid and cost-effective testing [22–24]. These developments indicate that the integration of LSPR into sensor technology will persist in enhancing the sensitivity and specificity of sensors in a diverse array of applications, such as environmental monitoring and medical diagnostics [25–27].

Much research has been done on the application of the functionalization of metal nanoparticles. However, the study about the coordination between organic molecules on metal nanoparticles has not yet been studied in detail. For this reason, a detailed study on the coordination between capping molecules (citrate and 3-MPA) and silver core (AgCA and AgMPA) was attempted through experimental and computational approaches. Moreover, in the application as a sensor probe based on functionalized AgCA, colorimetric testing with the Biocytin-Avidin system was performed in the experiment.

METHOD

Materials

Trisodium citrate dihydrate ($\text{HOC}(\text{COONa})(\text{CH}_2\text{COONa})_2 \cdot 2\text{H}_2\text{O}$, $M_w = 294.10$), 3-mercaptopropionic acid (3-MPA) 99% ($\text{HSCH}_2\text{CH}_2\text{CO}_2\text{H}$, $M_w = 106.14$, $\rho = 1.218\text{g/mL}$ at 25°C), and silver nitrate (AgNO_3 , $M_w = 169.87$) are purchased from Sigma-Aldrich. All materials are used directly without any purification process. Biocytin ($\text{C}_{16}\text{H}_{28}\text{N}_4\text{O}_4\text{S}$, $M_w = 372.48$) provided by Sigma-Aldrich and Avidin ($M_w = 66\text{ kDa}$) provided by Merck are used for colorimetric assay.

Synthesis of Silver Nanoparticles

Our previous report was followed to synthesize metal nanoparticles by used of chemical reduction method [28]. The citrate-capped silver nanoparticles (AgCA) used trisodium citrate dihydrate as a reducing agent as well as a capping agent, while the MPA-capped AgNPs (AgMPA) used trisodium citrate dihydrate as a reducing agent and 3-MPA as capping agent.

The synthesis of AgCA was prepared by dissolving metal salt in water. The precursor solution was heated and stirred in a three-neck flask using mantle heating. When the temperature of the solution reached boiling point, the trisodium citrate solution was added to the precursor solution. The solution was kept stirring until the color changed from transparent to yellow-brownish color, indicating the formation of nanoparticles. Meanwhile, the AgMPA was

prepared by dissolving metal salt in water. The precursor solution was heated and stirred until the temperature of the solution reached boiling point. Then, the trisodium citrate dihydrate and 3-MPA mixture was added to the precursor solution. The solution was kept stirring until the color of the solution changed. All the solutions were purified using the centrifugation method to remove extra citrate and 3-MPA. The final colloidal solution was stored at 4 °C for further use.

Colorimetric Assay

The colorimetric assay was conducted using biocytin-functionalized AgCA. First, AgCA was mixed with 10^{-4} M biocytin from Sigma-Aldrich and then incubated at room temperature. Tests were carried out by adding various concentrations of avidin to biocytin-functionalized AgCA.

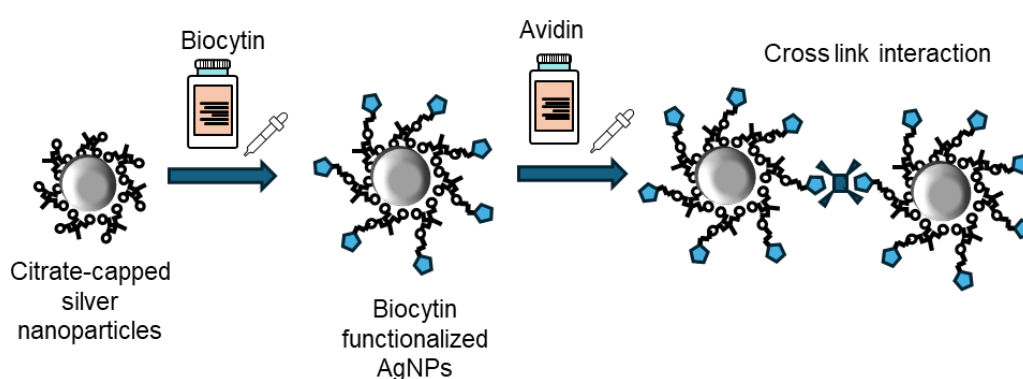


FIGURE 1. Colorimetric assay of AgCA using the biocytin–avidin system.

Characterization

Transmission Electron Microscopy (TEM) was performed to capture the morphology of the synthesized AgNPs, while UV-vis spectrometer was used to determine the optical properties of AgNPs. Then, Fourier Transform Infrared (FTIR) spectroscopy was conducted to investigate the coordination of capping molecules on the metal core in comparison to the capping molecule. In addition, vibrational analysis by DFT simulation was executed using the ORCA package version 4.2.1 to confirm the bonding between the capping molecule and the metal core.

RESULTS

The silver nanoparticles products (AgCA and AgMPA) revealed the specific solution color of transparent yellow-brownish, as shown in the insert of FIGURE 2. The plasmonic peaks in FIGURE 2, at around 418 nm for AgCA and 426 nm for AgMPA, indicate the formation of silver nanoparticles in the solution. The morphology of metal nanoparticles is predominantly spherical, as shown in FIGURE 3, with diameters of about 14 nm and 20 nm for AgCA and AgMPA, respectively.

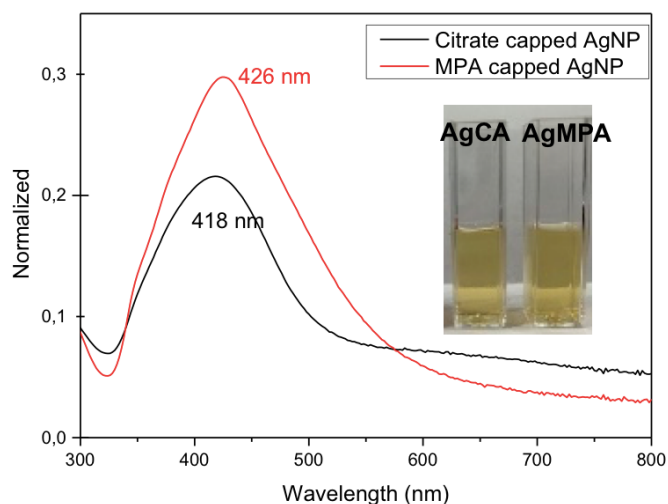


FIGURE 2. UV-Vis spectra of colloidal AgCA and AgMPA (inset: solutions of AgCA and AgMPA).

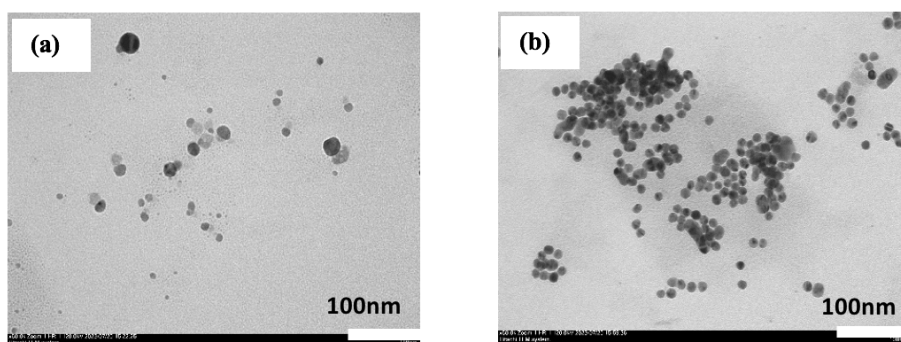


FIGURE 3. TEM images of (a) AgCA and (b) AgMPA.

Trisodium citrate is commonly used as a reducing agent and capping agent on metal nanoparticles, while the thiol end group of 3-mercaptopropionic acid (3-MPA) can adsorb easily on the metal surface via M-S bonds, and its carboxylic acid end group can contribute to surface functionalization of the metal. In the computational method, sodium bicarbonate was chosen as a simple substitute for the trisodium citrate structure, and the free 3-MPA structure was used to coordinate with the Ag ion.

FIGURE 4 shows the FTIR spectra of AgCA in comparison to those of trisodium citrate (CA) and Ag-bicarbonate (AgBic). The COO^- asymmetric stretching ($\nu_{\text{asym}} \text{COO}^-$) position is at 1591 cm^{-1} in free citrate, shifting slightly to a higher frequency in AgCA at 1595 cm^{-1} . In contrast, the COO^- symmetric stretching ($\nu_{\text{sym}} \text{COO}^-$) position shifts to a lower frequency, from 1400 cm^{-1} to 1382 cm^{-1} . However, the computational results reveal that the $\nu_{\text{asym}} \text{COO}^-$ position of AgBic shifts to a lower frequency from 1591 cm^{-1} to 1517 cm^{-1} , which is contrary to the experimental result. Environmental effects during measurement should be considered as one of the factors causing differences in the results. The computational method applies measurements under vacuum conditions, whereas FTIR spectroscopy data were collected in air and at room temperature. Another possible explanation for these results is the existence of the localized surface plasmon resonance (LSPR) effect from AgNPs, which is not taken into account in the simulation.

In this study, the FTIR spectra reveal that the peak of $\nu_{\text{sym}} \text{COO}^-$ is sharper than that of $\nu_{\text{asym}} \text{COO}^-$. This can be explained by the ionic bond between the carboxylate part of the capping material and the silver core. In agreement with the computational results in the inset of FIGURE 4, the coordination between the capping material and the Ag core is formed by the attachment of two oxygen atoms from the carboxylate to the Ag ion, resulting in an ionic bond. The details of the FTIR spectral assignments for AgCA are tabulated in TABLE 1.

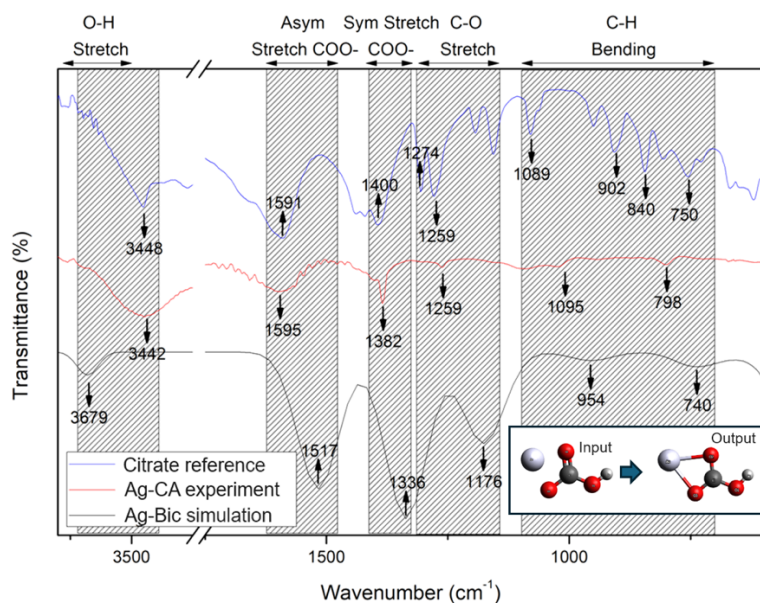


FIGURE 4. FTIR spectra of experimental AgCA and simulated Ag-Bic in comparison to the citrate reference (inset: computational results of the initial and final Ag-citrate configurations).

TABLE 1. Band assignments of experimental AgCA and simulated Ag-bicarbonate in comparison to the citrate reference.

Wavenumber (cm ⁻¹)				Band Assignment
CA Reference	AgCA Experiment	Ag-Bic Simulation		
750–1089	798–1095	740–954		C–H bending
1259–1274	1259	1176		C–O stretching
1400	1382	1336		COO ⁻ symmetric stretching
1591	1595	1517		COO ⁻ asymmetric stretching
3448	3442	3679		O–H stretching

In the case of AgMPA, in comparison to 3-MPA and the AgMPA simulation, the FTIR spectra show that the S–H bond from the 3-MPA molecule is located at 2573 cm⁻¹, but this peak disappears when 3-MPA interacts with Ag. The disappearance of the S–H bond indicates the formation of S–metal bonds, caused by the strong affinity of the thiol group to the metal surface (inset: FIGURE 5). The FTIR data of 3-MPA exhibit asymmetric and symmetric COOH stretching at 1708 cm⁻¹ and 1400 cm⁻¹, respectively. In AgMPA, the stretching of the carboxylic acid groups shifts to a lower frequency, and this experimental result agrees with the computational result. In contrast, the asymmetric COOH stretching of AgMPA is slightly

shifted to a higher frequency compared to the 3-MPA reference. This difference is attributed to the nanoparticles' plasmonic effects, which are not included in the computational modeling. The details of the FTIR spectral assignments for AgMPA are tabulated in TABLE 2.

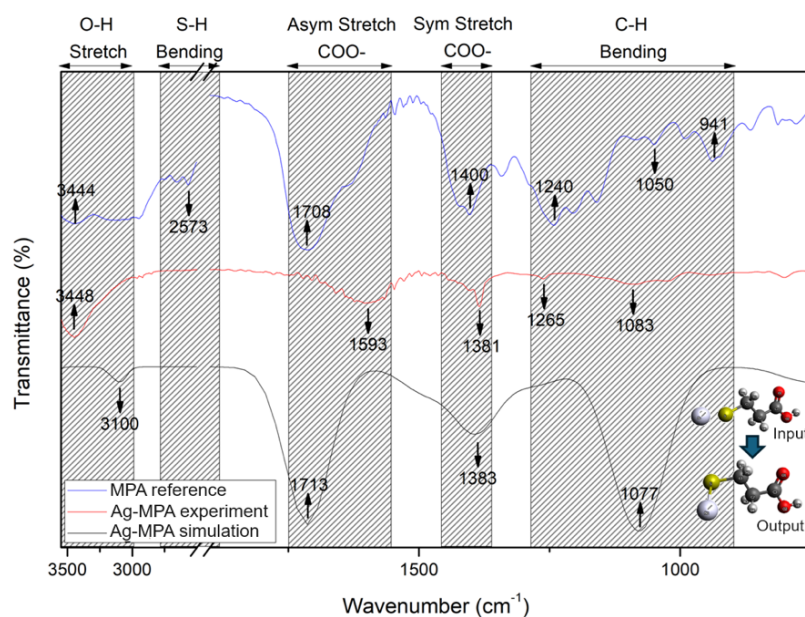


FIGURE 5. FTIR spectra of experimental AgMPA and simulated Ag-MPA in comparison to the 3-MPA reference (inset: computational results of the initial and final Ag-MPA configurations).

TABLE 2. Band assignments of experimental and simulated AgMPA in comparison to the 3-MPA reference.

Wavenumber (cm ⁻¹)			
MPA Reference	Ag-MPA Experiment	Ag-MPA Simulation	Band Assignment
941–1240	1083–1265	1077	C–O stretching
1400	1381	1383	COOH symmetric stretching
1708	1593	1713	COOH asymmetric stretching
1444	3448	3639	O–H stretching

Colorimetric tests were carried out on AgCA functionalized with biocytin as the probe, and avidin was used as the analyte. Biocytin is a water-soluble protein, and avidin is a tetrameric protein with a high affinity for biotin derivative molecules such as biocytin. The mechanism used in this colorimetric test is based on the interaction between biocytin and avidin, leading to cross-link aggregation [28], [29]. The addition of avidin at concentrations of 5–50 nM resulted in a shift in the LSPR peak of the functionalized AgCA. However, in this experiment, the color change in the AgCA solution was insignificant, as shown in FIGURE 6.

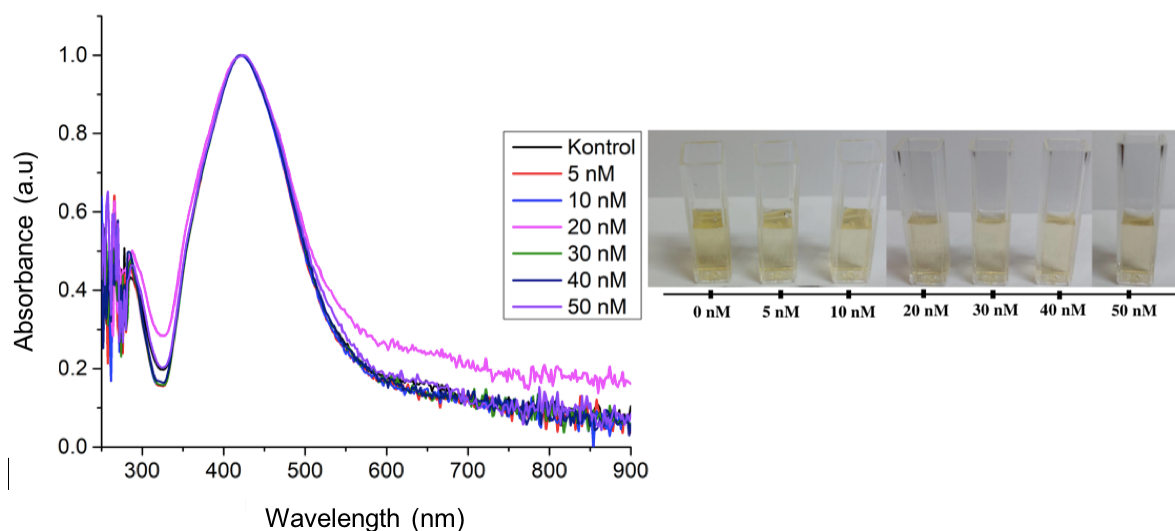


FIGURE 6. Absorbance spectra and qualitative observations of various avidin concentrations tested in the biocytin-functionalized AgCA colorimetric assay.

SUMMARY

In this work, citrate-capped silver nanoparticles (AgCA) and MPA-capped silver nanoparticles (AgMPA) were successfully formed in a spherical shape with diameters of approximately 14 nm for AgCA and 20 nm for AgMPA. The plasmonic peaks of AgCA and AgMPA colloids appeared at wavelengths of 418 nm and 426 nm, respectively, consistent with the results of a previous report. A coordination study of the capping materials (citrate and 3-MPA) on Ag metal indicated slight differences in the vibrational peak positions of chemical coordination, suggesting the effects of strong chemical bonding and localized surface plasmon resonance. In this case, the coordination of carboxylate from citrate with Ag forms an ionic bond, while the sulfur ion from 3-MPA forms a covalent bond. The experimental results also agree with the DFT-based calculations, which show similar trends in the vibrational peak positions. The colorimetric sensor test based on biocytin–avidin interaction shows a shift in the plasmonic peak of AgCA, although visible color changes were not observed.

ACKNOWLEDGEMENTS

This work was supported by Program Penelitian Kemendikbudristek, Skema PPS-PDD, Contract No.: 036/E5/PG.02.00.PL/2024 and derivative Contract No: 241/IT1.B07.1/SPP-LPPM/VI/2024.

REFERENCES

- [1] B. Oliveira, D. Ferreira, A. Fernandes, and P. Baptista, “Engineering gold nanoparticles for molecular diagnostics and biosensing,” *Wiley Interdiscip. Rev. Nanomed. Nanobiotechnol.*, vol. 15, no. 1, 2022. doi: 10.1002/wnan.1836.
- [2] Y. Dutt *et al.*, “Therapeutic applications of nanobiotechnology,” *J. Nanobiotechnol.*, vol. 21, no. 1, 2023. doi: 10.1186/s12951-023-01909-z.
- [3] Z. Dang, X. Ma, Z. Yang, X. Wen, and P. Zhao, “Electrospun nanofiber scaffolds loaded with metal-based nanoparticles for wound healing,” *Polymers*, vol. 16, no. 1, p. 24, 2023. doi: 10.3390/polym16010024.

- [4] N. Rawat *et al.*, “Nanobiomaterials: exploring mechanistic roles in combating microbial infections and cancer,” *Discover Nano*, vol. 18, no. 1, 2023. doi: 10.1186/s11671-023-03946-x.
- [5] Y. Shang *et al.*, “Gold nanoparticle-based biosensors for bacterial detection,” *Sensors*, vol. 23, no. 3, p. 1211, 2023.
- [6] Y. Zhou, S. Wang, A. Rodriguez, and M. Zaghoul, “Development of liquid-phase plasmonic sensor platforms for prospective biomedical applications,” *Sensors*, vol. 24, no. 1, p. 186, 2023. doi: 10.3390/s24010186.
- [7] J. Bocarando-Chacon *et al.*, “Unraveling of poly(lactic acid) (PLA)/natural wax/titanium dioxide nanoparticle composites for disposable plastic applications,” *Polymers*, vol. 17, no. 5, p. 685, 2025. doi: 10.3390/polym17050685.
- [8] C. Cao, A. Killips, and X. Li, “Advances in the science and engineering of metal matrix nanocomposites: a review,” *Adv. Eng. Mater.*, vol. 26, no. 20, 2024. doi: 10.1002/adem.202400217.
- [9] C. Comanescu, “Recent advances in surface functionalization of magnetic nanoparticles,” *Coatings*, vol. 13, no. 10, p. 1772, 2023. doi: 10.3390/coatings13101772.
- [10] S. Yasmin *et al.*, “Magnetic nanofluids: synthesis, properties and applications in energy systems,” *J. Mol. Liq.*, vol. 387, 2023.
- [11] Y. Liu *et al.*, “Localized surface plasmon resonance of metal nanoparticles and its applications,” *Nano Today*, vol. 9, pp. 396–416, 2014.
- [12] J. Zhang *et al.*, “Gold nanoparticles and their LSPR properties for biosensing applications,” *Biosensors*, vol. 7, no. 3, p. 49, 2017.
- [13] B. Mahjub *et al.*, “Colorimetric detection of tobramycin using aptamer-conjugated silver nanoparticles,” *Sens. Actuators B Chem.*, vol. 360, 2022.
- [14] A. Negi, “LSPR-based sensing using silver nanoparticles: recent advances,” *Sensors Int.*, vol. 3, p. 100156, 2022.
- [15] D. Polte, “Fundamental growth principles of colloidal metal nanoparticles – a new perspective,” *CrystEngComm*, vol. 17, pp. 6809–6830, 2015.
- [16] X. Hu *et al.*, “Influence of dielectric medium on LSPR characteristics of gold nanoparticles,” *Nanoscale Res. Lett.*, vol. 16, 2021.
- [17] Y. Wang *et al.*, “Citrate-capped nanoparticles for biomedical applications: stability and functionality,” *Colloids Surf. B Biointerfaces*, vol. 211, p. 112296, 2022.
- [18] R. Jin *et al.*, “Functionalization of metal nanoparticles with capping agents,” *Chem. Rev.*, vol. 123, pp. 218–250, 2023.
- [19] R. Sekar *et al.*, “Colorimetric sensing of bacteria using glucose-functionalized gold nanoparticles,” *Anal. Chem.*, vol. 95, no. 4, pp. 1561–1568, 2023.
- [20] J. Park *et al.*, “Uniform gold nanostructure formation via weakly adsorbed gold films and thermal annealing for reliable LSPR-based detection of DNase-I,” *Small*, vol. 19, no. 39, 2023. doi: 10.1002/sml.202302023.
- [21] S. Sun *et al.*, “Plasmonic biosensors using gold nanorods and nanoshells,” *Biosensors*, vol. 14, 2024.
- [22] Y. Cui, J. Zhao, and H. Li, “Chromogenic mechanisms of colorimetric sensors based on gold nanoparticles,” *Biosensors*, vol. 13, no. 8, p. 801, 2023. doi: 10.3390/bios13080801.
- [23] S. Dandu, D. Joshi, T. Park, and S. Kailasa, “Functionalization of gold nanostars with melamine for colorimetric detection of uric acid,” *Appl. Spectrosc.*, vol. 77, no. 4, pp. 360–370, 2023. doi: 10.1177/00037028231154935.
- [24] P. Preechaburana, S. Sangnuy, and S. Amloy, “Paper-based colorimetric sensor for mercury ion detection using smartphone digital imaging,” *J. Met. Mater. Miner.*, vol. 33, no. 2, pp. 81–87, 2023. doi: 10.55713/jmmm.v33i2.1653.
- [25] L. Kim *et al.*, “Recombinant protein embedded liposome on gold nanoparticle based on LSPR method to detect coronavirus,” *Nano Converg.*, vol. 10, no. 1, 2023. doi: 10.1186/s40580-023-00399-x.
- [26] S. Sayın *et al.*, “Development of liquid-phase plasmonic sensor platforms for prospective biomedical applications,” *Sensors*, vol. 24, no. 1, p. 186, 2023. doi: 10.3390/s24010186.

- [27] A. Galiutdinov and Y. Zhao, "Plasmonic properties of composition graded spherical nanoparticles in quasi-static approximation," *J. Phys. D: Appl. Phys.*, vol. 56, no. 5, p. 055102, 2023. doi: 10.1088/1361-6463/acad8a.
- [28] M. T. Pambudi, A. Hardianto, M. Yusuf, and P. Wulandari, "Localized surface plasmon effect on 3-mercaptopropionic acid and citrate stabilized gold nanoparticles for biosensor application," *J. Nonlinear Opt. Phys. Mater.*, vol. 31, no. 4, Dec. 2022. doi: 10.1142/S0218863523500042.
- [29] S. Rahayu, A. Labiba, Herman, and P. Wulandari, "Localized surface plasmon resonance effect of 3-mercaptopropionic acid capped on silver nanoparticles for sensing probe application," *J. Phys.: Conf. Ser.*, vol. 2696, no. 1, p. 012014, 2024. doi: 10.1088/1742-6596/2696/1/012014.